

# Image collection and processing system for welding pool and proximate seam using multiple image detectors

Yanming Quan, Qilin Bi\*

*School of Mechanical and Automotive Engineering, South China University of Technology, Guangzhou, Guangdong 510640 China*

*Received 1 October 2014, www.cmnt.lv*

---

## Abstract

Because of the dynamic nature of welding parameters and power characteristics, the arc ignites and extinguishes too rapidly. The length and luminous intensity of the arc is unstable. This makes the imaging of the welding pool and seam problematic for selecting and fixing time of exposure for the camera. Moreover, the luminous intensity of region being welded decreases sharply along the welding seam. The seam that is not in the proximity of the welding pool is too dim for imaging by the camera, making the length of the seam imaged too short. In this study, an image-capturing system based on multiple image detectors and image fusion are used to image the welding pool and proximate seam during MAG welding process. The offset between center point of the welding pool and center line of seam and the seam width are determined by innovative measuring techniques that include collection of images of the pool and seam using multiple image detectors. The results obtained have shown that the accuracy of offset between welding pool and seam is  $\pm 0.5\text{mm}$ , and the accuracy of seam width is  $\pm 0.5\text{mm}$ . This imaging and measuring method developed in this study is promising for tracking and monitoring of high-speed welding, especially the MAG welding where interference from the arc is a problem.

*Keywords:* MAG automatic welding, welding seam tracking, multiple image detectors, image fusion

---

## 1 Introduction

In the manufacturing of containers, railway coaches and other large work-pieces involving welding, the length of corrugated seam reaches tens of meters, and the position and width of assembly gap to be weld become irregular. To control and maintain high quality of welding, the manufacturing industry is in a great need for efficient, precise, reliable, intelligent automatic welding equipment. With the development of computers and sensor technology, tracking and monitoring welding seam have become an active area of research in automatic welding field.

Currently, some welding tracking and monitoring methods (eye recognition, direct copy, arc sensor, laser sensor, electromagnetic sensor, etc.) are used to the track welding trajectory and guide the torch motion. The Eye recognition cannot be used in automatic welding. The direct copy method is simple, and economical, but wears out easily, and is subject to the positional limitations. The arc sensor is accurate and well established in usage, but unfixed welding parameters and bevelled edges reduce its performance. The non-contacting electromagnetic sensor is resistant to abrasion, but is suitable only when bevelled edges are symmetrical. All the above techniques which are applied in some special situations can recognize only the weld seam trajectory and not the seam width. If welding parameters are fixed during welding process of thin work-pieces like a container, it is certain that some parts of seam are not welded fully while some parts of the material are melted through.

During the recent years, the method of laser line has become an active area of research and also its application. The technique of ranging with the laser point has some beneficial effects in guiding the torch to follow the assembly seam trajectory, but its precision is limited, especially in obtaining tridimensional locations of the assembly seam trajectory. A more common method is to project a laser line to recognize welding seam [1-3]. In this technique one or more laser lines are projected in front of the welding area a camera is made to capture image of laser line modulated by the assembly seam being welded, then line segments are extracted from the captured image and the location of the middle line and width of the seam are acquired. However, to avoid the interference from arc light, it is necessary to project the laser lines at some distance from the welding area which imposes limitation on the accuracy. Moreover, the errors caused by thermal deformation, mechanical error etc. are difficult to predict.

There have been research efforts to reduce the interference of arc light so that the laser lines are projected nearer to the welding area. In their studies, Jae Seon Kim et al. [4] used a mirror to change the optical path of a vertically installed laser, so that laser line is projected closer to the welding pool at an angle. In addition, an optical filter of narrow band (the central wave length is same as the wave length of laser and the width of passing band is 10nm) is installed in front of Charge-coupled Device (CCD). The image of the laser line modulated by seam in front of the welding pool is acquired to recognize and track the assembly seam, and the advance error is lowered to some degree.

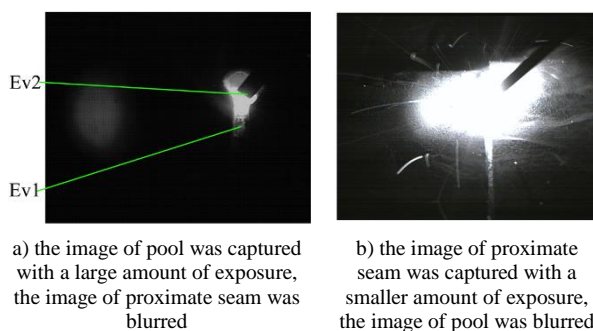
---

\* *Corresponding author's* e-mail: bi.qilin@mail.scut.edu.cn

Image detectors can be used to directly acquire the image of welding pool and proximate assembly seam. Using this method, the position of torch tip, position and width of seam, offset between the torch tip and seam middle line, etc. can be extracted, and transferred to control system to adjust the torch motion trajectory and welding parameters. In this way, the advance error is eliminated. However, serious interferences such as strong arc, protective gas, splash slag, etc. still exist. The difficulties mainly are the following.

1) The light intensity dynamic range (LIDR) is too large to fit the camera. As a result of strong arc, the LIDR ( $E_{v1}/E_{v2}$ ) of the whole region of the pool (where average light intensity is  $E_{v1}$ ) and seam (where average light intensity is  $E_{v2}$ ) reaches hundreds of db. The dynamic range of common CCD is about 40-60dB. If a small exposure is used, the region where the light intensity is between  $E_{v1}/60$  and  $E_{v1}$  can be clearly imaged, but the region being welded where the light intensity is low and is in complete darkness, as shown in Figure 1a. If a larger exposure is used by the camera, the region where the light intensity is between  $E_{v2}$  and  $60 \cdot E_{v2}$ , the image obtained is clearly visible; the region where light intensity is between  $60 \cdot E_{v2}$  and  $E_{v1}$ , the electrons of CCD pixels overflow making the appearance of the image completely white as shown in Figure 1b.

2) Strong arc light and diffusing proactive gas make it difficult to acquire a steady and clear image. The arc light is ignited and then extinguished because the welding power is in form of pulse. If the camera uses a fixed exposure to capture the image, the acquired image depending on time is clear or obscure as shown in Figures 1a, and 1b. The proactive gas diffusing around the welding pool also influences the imaging process. It is difficult to extract reliable information from unstable images so produced.



a) the image of pool was captured with a large amount of exposure, the image of proximate seam was blurred

b) the image of proximate seam was captured with a smaller amount of exposure, the image of pool was blurred

FIGURE 1 The image of pool and proximate seam under different exposure

3) The length of seam in image is short. The optical filter and dimmer installed in front of the CCD prevent the interference of arc light to capture image of the region of strong light. However, the luminous intensity of the region being welded decreases sharply along the welding seam, causing the region away from the welding pool not to be imaged. The recognized seam should be long enough, so that the offset between torch and middle line of the seam

is calculated precisely, and the control system is given time to adjust the trajectory of torch and the welding parameters.

The quality of imaging of welding area is improved successfully, by large amount of research in the past. The most common method is to using an optical filter. Based on welding technology, a specific optical filter is so selected that it allows wave band in which the arc light intensity is low to pass through and rejects the rest of the wave band. For example, S. Chokkalingham et al. [5] used an optical filter of 499-511 nm in TIG welding of stainless steel. Gao X.D. et al. [6] used infrared camera and 960-990 nm optical filter made up of two pieces in laser welding of stainless steel. This method can reduce interference from arc light significantly and help to capture image of welding pool.

A dimmer installed in front camera can reduce interference of arc light further. Shen H. Y. et al. [7] added 590-710nm filter and 70%-99% dimmer to the vision system of GTAW welding. The depth of the field is enhanced by adjusting aperture of the camera, so that the quality of image is improved.

Xu Y. L. et al. [8-10] used two parallel mirrors in the vision system designed for GTAW welding. This idea is similar to that of Jae Seon Kim et al. [4]. After reflecting twice by mirrors, the image of welding pool passes through a filter of 660-680nm and a dimmer of 90%, and finally is captured by the camera. This method helps in avoiding the need for the camera to be nearer to the welding area to capture image directly. Further splashing the camera by slag is also prevented.

By illuminating the region in front of the welding pool by an auxiliary light of high intensity, the difference between the luminous intensity of this region and the welding pool can be decreased. So that an improved image of the welding pool and the proximate region can be captured. In the automatic seam tracking system designed by Shi Y. H. et al. [11] for underwater flux-cored arc welding, halogen lights (50w) are used to illuminate the region in front of welding pool. The CCD supported by filter and dimmer is used to capture the image of the welding pool and the region being welded. However, the larger the region to be illuminated the higher is the power of auxiliary light. This makes the cooling of auxiliary light a problem.

A camera of higher dynamic range can significantly improve the quality of the image of the welding pool and the proximate region. Photon Focus Company in Switzerland developed a camera of wide LIDR (120dB) using Linlog technology. This technology compresses the response of saturated region or region close to saturation and keeps the sensitivity and linearity of low illumination region in the image. Based on this technology, Li M. X. et al. [12] captured the image of seam and pool in low carbon steel short circuit transition welding process.

To summarize, an ordinary camera assisted with optical filter and dimmer can capture a clear image of the welding pool; an auxiliary light of high intensity

illuminating the region to be welded can improve the quality of image further. However, during process of MAG welding, the problem of flickering arc light is serious. With all the above methods it is still difficult for ordinary camera of fixed exposure parameter to capture clear image of welding pool and proximate region in the same field of view at the same time. The quality of successive images is not uniform. To solve this problem, this study proposes a method of using multiple image detectors to capture the image of automatic MAG welding. Two cameras of different exposure parameters will be setup to synchronically capture the images. One camera captures the image of the welding pool and the other the image of front region. The images obtained will be fused and processed. After this process, the width of welding seam and the offset between welding pool center and center line of seam will be determined dynamically.

**2 Visual systems based on multiple image detectors**

Dual cameras with different exposure parameters simultaneously capture images of the same object (pool and seam). Then, the images from two source-channels are fused and processed. The information of images from each channel is used effectively. The image capturing and processing experimental system is composed of imaging device (camera mounting box, two cameras, beam splitting lens, optical filter, diffuse-cutting filter, etc.), auxiliary light source, work-piece motion platform, welding equipment, etc., as shown in Figure 2a. The imaging device is shown in Figure 2b.

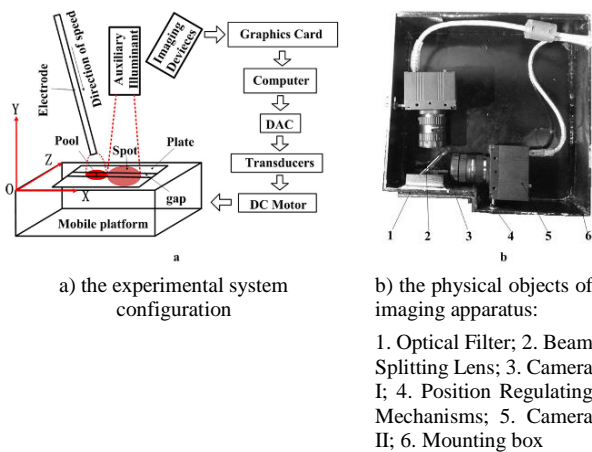


FIGURE 2 The experimental system

In this experimental system, the plate to be welded is on the motion platform (Weld seam is along the *x*-axis). The motion platform driven by a motor moves in *xz* plane. The welding torch and visual system are fixed. The welding torch, auxiliary light, and the vision system are fixed in the *xy*-plane. The angle between the axis of welding torch and the normal vector of the plate is 15° (to avoid blocking the view for the camera). The axis of auxiliary light is vertical to the plane of welding structure, and its top is 400mm away from the plane along *Y* axis.

The auxiliary light which is used to illuminate the region in front of welding pool forms a bright disc. After the image of interesting region (IR) AB where LIDR is high passes through the optical filter and the beam splitting lens (the plane of the beam splitting lens formed a 15° angle with the plane of optical filter), two enantiomorphism images are formed. The camera I of smaller exposure captures the image A'. The camera II of larger exposure captures the image B'. By using appropriate algorithms the image A'B' is fused and the information about the region of interest is extracted by the software LabVIEW 2010.

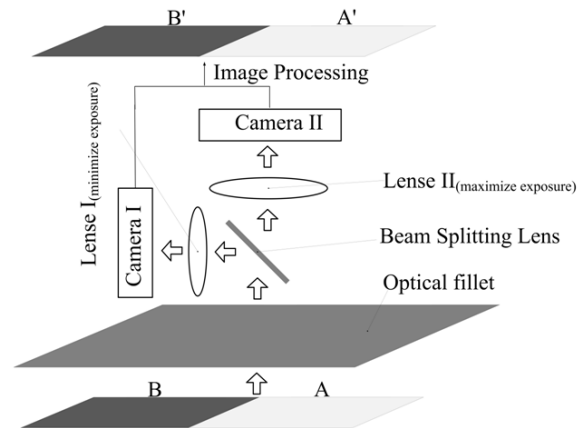


FIGURE 3 The principle of capturing images which the light intensity dynamic range was too large: A represent region with a larger illumination; B represent region with a small illumination

**3 The filter and exposure**

In welding process, the optical signal of the pool and seam consists of three parts: arc light, thermal radiation from pool, and auxiliary light reflected by the seam. The thermal radiation *t* of pool is used to image the pool; the auxiliary light is used to image seam. In the process of capturing the image of pool and seam, optical methods such as optical filter, auxiliary light, and controlling exposure are useful to suppress the interference of the strong arc.

**3.1 THE OPTICAL FILTER**

The spectrum of arc includes all wavelengths of visible light. It has highlight intensity, which leads to some parts of region of interest to be shaded by the arc and LIDR to be too large. The light distribution of arc, pool, and the seam are presented in Figure 4.

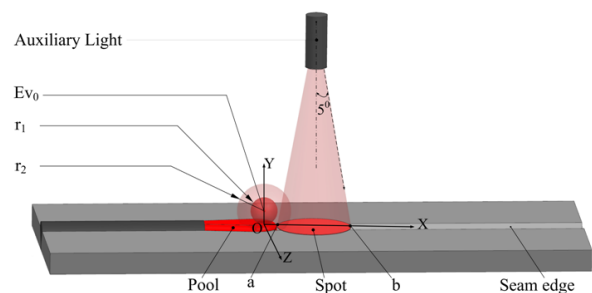


FIGURE 4 The light distribution of interesting region

It is assumed that arc is a point light source, and the exposure of camera is fixed. The notation for arc light intensity is  $Ev_0$ . When the optical filter is not used, the radius of the arc image is  $r_1$  and some part of IR is blocked. When the optical filter is used, the attenuation rate of arc light intensity is  $\eta_0$  ( $\eta_0 < 1$ ). Under this condition, the radius ( $r_2$ ) of the arc image is given by the following relationship:

$$\frac{r_2^2}{r_1^2} = \frac{(1-\eta_0) \cdot Ev_0}{Ev_0}$$

Also

$$r_2 = (1-\eta_0)^{\frac{1}{2}} \cdot r_1 \tag{1}$$

Therefore, a higher attenuation rate  $\eta_0$  can make the image clearer and avoid blocking IR. Bao S.D. et al. [13] studied the arc spectrum distribution in MAG welding process ( $\varphi$  (CO<sub>2</sub>) 20% +  $\varphi$  (CO<sub>2</sub>) 80%), and their results are shown in Figure 5. Under the condition of a welding current of 150A, 200A, or 300A, the light intensity at 650 nm is found weakest and relatively stable. Hence, an optical filter whose center wavelength is 650nm can make the attenuation rate higher and more stable.

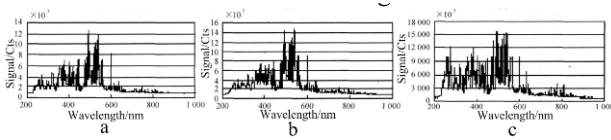


FIGURE 5 Arc spectrum distribution of MAG welding [13]: a) the welding current was 150A; b) the welding current was 200A; c) the welding current was 250A

### 3.2 THE AUXILIARY LIGHT

The distance between the arc center and the point  $a$  (where the seam and the pool intersect) is  $h_0$  along  $y$ -axis and  $L_0$  along  $x$ -axis separately. The length of identified seam in image is  $L$ , as shown in Figure 4. In the absence of auxiliary light, the illuminance at point  $a$  and  $b$  is given by the following Equations:

$$\begin{cases} Ev_a = \frac{Ev_0}{h_0^2 + l_0^2} \\ Ev_b = \frac{Ev_0}{h_0^2 + (L+l_0)^2} \end{cases} \tag{2}$$

The LIDR of camera is assumed as  $dB$ . In order to image the target clearly, the following condition should be satisfied:

$$dB \geq \frac{Ev_a}{Ev_b}$$

Also

$$L \leq (dB(h_0^2 + l_0^2) - h_0^2)^{\frac{1}{2}} - l_0 \tag{3}$$

With an auxiliary light, the illuminance at points  $a$  and  $b$  is assumed as  $Ev_1$ . Then the total illuminance at points  $a$  and  $b$  is as follows:

$$\begin{cases} Ev'_a = \frac{Ev_0}{h_0^2 + l_0^2} \\ Ev'_b = \frac{Ev_0}{h_0^2 + (L+l_0)^2} \end{cases} \tag{4}$$

Using the Equations (3) and (4), Equation (5) for the length ( $L'$ ) of the recognized seam is obtained. The length  $L'$  can now be calculated as

$$L' \leq (dB(h_0^2 + l_0^2) - h_0^2)^{\frac{1}{2}} - l_0 \cdot \frac{1}{1 - \frac{Ev_1}{Ev_0}(dB-1)(h_0^2 + l_0^2)} \tag{5}$$

Also

$$\begin{cases} \frac{Ev'_a}{Ev'_b} < \frac{Ev_a}{Ev_b} \\ L'_{max} > L_{max} \end{cases} \tag{6}$$

Therefore, the auxiliary light can reduce the LIDR of IR and increase the length of recognized seam. In the capturing process, low and declining light intensity and high power LED (composed of 4 LED of 3W, 80 Liu and the 650 nm center wave) is used. The light illuminated the seam in front of pool at a 5° angle and produced a highly bright spot, as shown in Figure 4

### 3.3 THE EXPOSURE OF TWO SYNCHRONIZED CAMERAS

The quantity of exposure  $Hv$  depends on time of exposure and illuminance at CCD surface,  $Ev$ . When an object is captured by the camera, the illuminance at CCD surface is proportional to the aperture size  $f$ . The relationship between the quantity of exposure, time of exposure and aperture size is as follows.

$$Hv = Ev \cdot t = K \cdot f \cdot t \tag{7}$$

$(0 \leq f \leq F)$

$K$  is proportion of illuminance  $Ev$  to aperture size  $f$  ( $lx/mm^2$ ),  $F$  is the max aperture size ( $mm^2$ ).

Since the two synchronized cameras require a quantity of exposure,  $Hv_0$  at least to capture clear images of IR, the exposure time should satisfy the following condition.

$$Hv_0 \leq K \times f \times t$$

Also

$$t \geq \frac{Hv_0}{K \cdot f} \tag{8}$$

During the time interval of driving signal  $T_0$ , the system has to complete the image capturing (the time needed is

approximately equal to the exposure time  $t$ , image processing ( $t_1$ ), and information transferring ( $t_2$ ) to continuously guide the torch. For completing these actions,  $T_0$  must satisfy the following condition:

$$T_0 \geq t + t_1 + t_2 .$$

Also

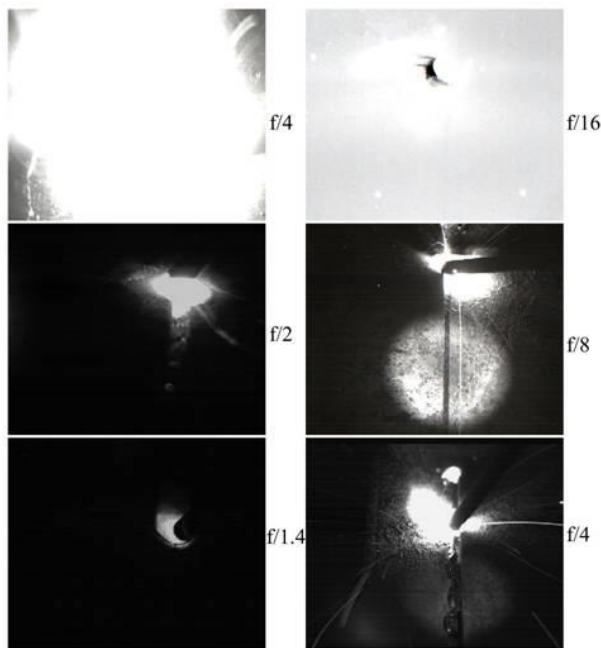
$$t \leq T_0 - t_1 - t_2 . \tag{9}$$

From the Equations (8) and (9), the relationship (10) is obtained:

$$\frac{Hv_0}{K \cdot f} \leq t \leq T_0 - t_1 - t_2 . \tag{10}$$

The experiments established that an exposure time of 1/20S meets the requirements.

Because of synchronized exposure of the cameras I and II, the only way to adjust the exposure is to change the aperture size. In the image acquisition process, the aperture sizes of cameras I and II are adjusted dynamically. The acquired images are shown in Figure 6.



a) the image of pool captured by camera I      b) the image of seam captured by camera II

FIGURE 6 The image under different value of exposure

The images obtained by the experiment showed that camera I with an aperture of f/2 and camera II with an aperture of f/8 can successfully capture high-quality images of pool and seam separately.

## 4 Extracting features of pool and proximate region

### 4.1 THE IMAGE PROCESSING

The image processing scheme of pool and proximate region are shown in Figure 7. The contour and coordinates of center of pool are extracted from the image A' captured by the camera I. The edges and center line of the seam are extracted from image B' captured by the camera II. The coordinates of feature parameters extracted from image A' of camera I are transformed to the image B' of camera II. The offset between the center of pool and the center line of seam is acquired through image fusion.

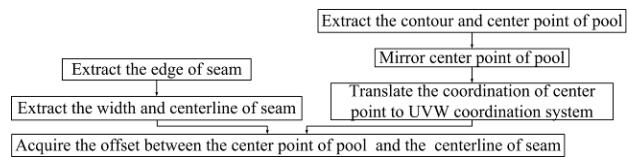
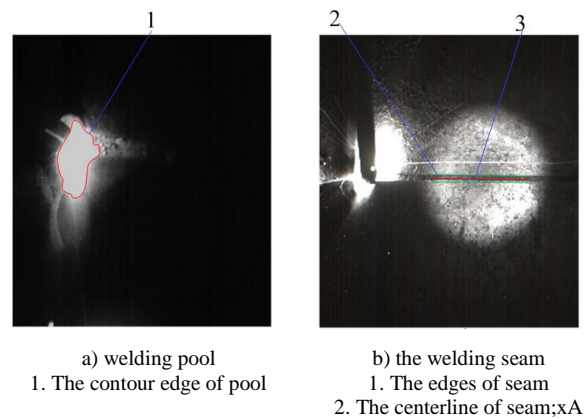


FIGURE 7 The scheme of image processing

### 4.2 EXTRACT CONTOURS FROM IMAGE

The features of pool contours and seam edges contain large information on work-piece (the offset between torch and seam, width of seam being welded, etc.). A well-considered strategy is necessary for identifying the features, reducing the error rate and improving the accuracy of detected position and for ensuring that only one edge is detected. For this purpose Canny sub-pixel edge detector is used to detect the contours of the pool and seam for obtaining the seam edge and center line, as show in Figure 8a.



a) welding pool      b) the welding seam  
1. The contour edge of pool      1. The edges of seam  
2. The centerline of seam;xA

FIGURE 8 The contour edge of pool and proximate seam

The polygon approximation method to extract contours is simple, fast, and avoids complex computation of the second derivative, etc. [14]. Therefore this method is used to extract the pool contour edge. In this study, through polygon approximation method, the pool contour edge is extracted from which the pool center is acquired as shown in Figure 8b.

4.3 FUSING THE IMAGE AND OBTAINING THE OFFSET

In the process of capturing images, the model and the field of view (both cameras adopted a+b) of the cameras I and II are the same. In RST image coordinates of camera I, the *t*-axis is optical axis of camera I and the origin *t* is at the center of CCD. In UVW image coordinates of camera II, the *w*-axis is the optical axis of camera II and the origin is at the CCD center of camera II. All these details are shown in Figure 9.

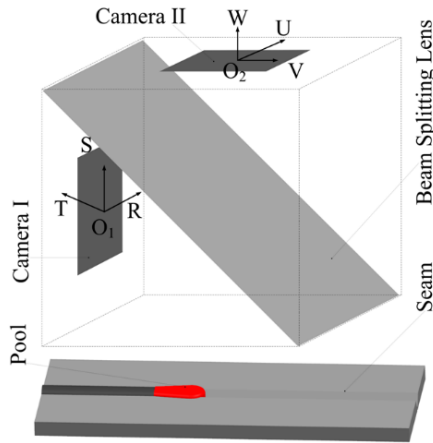


FIGURE 9 The coordinate relation in the image fusing process

Before starting the welding, the image of the wire tip (point O) is captured by both cameras at the same time. After image processing, the coordinate of point O ( $R_0, S_0$ ) in RST image coordinate system and the coordinate of point O ( $U_0, V_0$ ) in UVW image coordinate system are acquired separately. Their relationships can be expressed in the following form:

$$\begin{cases} R = U + (R_0 - U_0) \\ S = V + (S_0 - V_0) \end{cases} \quad (11)$$

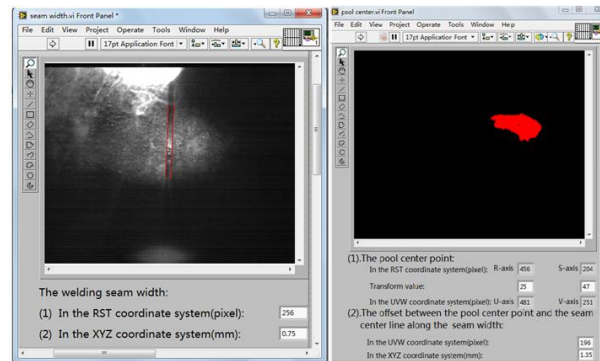
During the welding process, the image of pool is first reflected by a plane mirror and then captured by camera I with a smaller exposure. Subsequently the pool center ( $R_{pool}, S_{pool}$ ) is captured through the image processing. The Figure 9 shows that there is no change in the captured image of pool relative to the actual image of pool in *s*-axis direction. In *r* direction, it is turned around the *s*-axis. Therefore, the actual coordinates of the center of the pool ( $R'_{pool}, S'_{pool}$ ) in the RST image coordinate system are given by the following Equations:

$$\begin{cases} R'_{pool} = -R_{pool} \\ S'_{pool} = S_{pool} \end{cases} \quad (12)$$

The Equations (11) and (12) show that the coordinates of center point of pool ( $R''_{pool}, S''_{pool}$ ) in the UVW coordinate system can be expressed as follows:

$$\begin{cases} R''_{pool} = -R_{pool} + (R_0 - U_0) \\ S''_{pool} = S_{pool} + (S_0 - V_0) \end{cases} \quad (13)$$

According to Equation (13), the images of the same object captured simultaneously by the cameras I and II at the same time are fused. Then according to the calibration parameters, the offset between center point of the pool and center line of seam and the seam width are acquired through image processing. Using the LabVIEW 2010, the seam edges, center line and width are extracted and the results obtained are shown in Figure 10a; the pool contour and center point are extracted. Then, the information is fused into one image, and the offset between the pool center point and the seam center line is obtained as shown in Figure 10b.



a) the extraction of the seam width

b) the extraction of the offset between the center point of pool and the center line of seam

FIGURE 10 Image fusion and parameters extracting

5 Capturing image in the welding monitoring process

5.1 EXPERIMENTAL CONDITIONS

Butt MAG welding is designed to verify the viability, effectiveness of capturing and processing images of pool and proximate seam based on multiple image detectors. During the straight bead welding process of plate, if the welding torch moves along the seam center line, it is difficult to prove that this method can monitor the offset between the torch and the seam as the offset is not obvious. To clearly demonstrate the continuous change of offset in the tracking and monitoring process, a flexuous torch motion trajectory is designed. The material of work piece is 45 steel. The size of work piece and the welding trajectory are shown in Figure 11. The thickness of plate is 4mm.

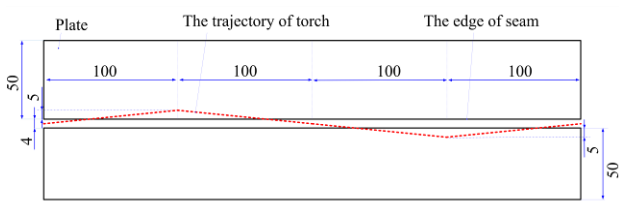


FIGURE 11 The size of work piece and welding torch trajectory (mm)

In the process of capturing the image, ARTCAM-130MI-DRV-V200 cameras, a computer, camera lens ( $f=25\text{mm}$ ), optical filter (the center wavelength: 650nm, the pass-band width: 32nm) are used. A flint glass (light transmittance $\geq 97\%$ ) is placed in front of the optical filter to protect it from splashing slag. The wire is fed by the torch fixed at the same position. The work piece is driven by the motion platform. The welding parameters are shown in Table 1.

TABLE 1 Parameters of welding

Name	Parameters
Welding wire diameter (mm)	$\phi 1.2$
Welding machine	NB-200 inverter welding machine
Welding speed (mm/s)	10
Welding current (A)	290-310
Welding voltage (v)	29-31
Welding groove	Plate butt welding
Material	45#
Thickness of plate (mm)	4
Extension of bole (mm)	400

## 5.2 EXPERIMENTAL RESULTS AND ANALYSIS

Vision system and related welding parameters are regulated before starting welding process. During the welding process, camera I and II captured the images of the pool and proximate seam separately. Then these images are fused, the result of which is shown in Figure 12.

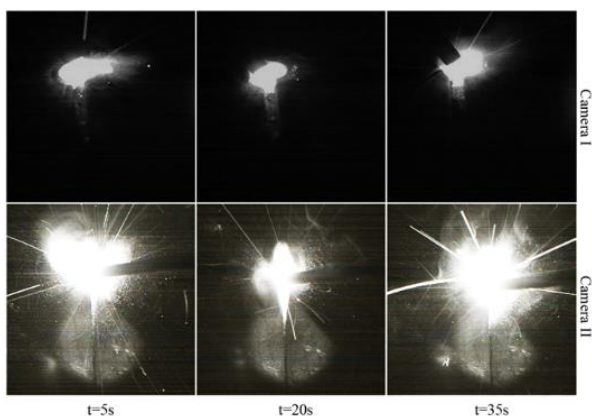


FIGURE 12 Image capturing in different cameras at same time

The parameters of seam are obtained by processing the image of seam, shown in Figure 13a. The curve 1 represents the assembly gap width planned (AGW-P)

along  $x$ -axis before starting of welding. The curve 2 represents assembly gap width monitored by virtual sensors (AGW-MVS) along  $x$ -axis during the welding process. The fused image is first processed, and then the welding trajectory is acquired, as shown in Figure 13b. The curve 1 represents torch trajectory planned (TT-P) before starting of welding (the seam center line is  $x$ -axis and the starting point of welding is the original point). The curve 2 represents the center point trajectory of pool monitored by visual sensors (CPTP-MVS) in the welding process.

The Figure 13a shows that AGW-MVS is generally in accordance with AGW-P (the error is approximately  $\pm 0.5\text{mm}$ ) and the value of assembled gap became smaller and tended to be stable during the welding process. This phenomenon is mainly caused by the high heat input. As pool is cooled, the assembled gap is narrowed by the shrinkage stress. Tack welding made the width of assemble gap to become stable.

The Figure 13b shows that CPTP-MVS is generally in accordance with TT-P (the error is approximately  $\pm 0.5\text{mm}$ ). This phenomenon is mainly caused by factors such as high heat input, curved wire, and arc blowing. First, TT-P is the trajectory of tip of wire that is not curved. However, the wire is curved into irregular form after it exited welding torch. This resulted in the difference between the true and the planned trajectories of the wire tips. Secondly, because of arc blow, the error existed between the center point of the pool and the projection point of wire tip on the plate. Hence, an error between CPTP-MVS and TT-P also existed.

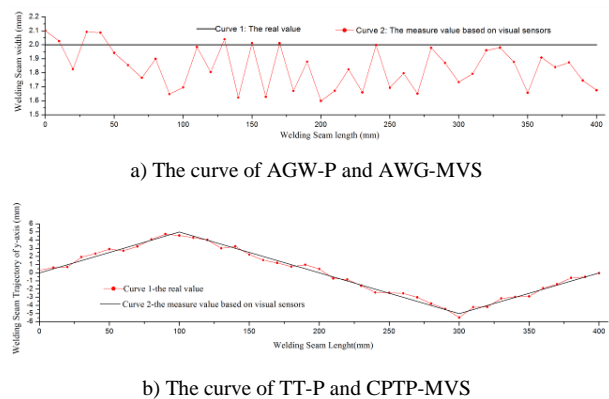


FIGURE 13 The curve of experiments results

## 6 Conclusions

The experimental results reported in this paper verify that: vision system based on multiple image detectors can capture stable and clear images of the welding pool and the proximate seam; the width of seam and the offset between center of pool and center line of the seam can be acquired by extracting features and fusing of images; these results can be used to adjust the welding parameters and guide torch motion on-line, to realize highly precise, efficient, intelligent welding process.

## Acknowledgments

The authors gratefully acknowledge the financial support from the key project of the strategic cooperation among

Guangdong Province and Chinese Academy of Science, 2013 (to be issued soon).

## References

- [1] Kim M Y, Ko K-w, Cho H S, Kim J-h 2000 Visual sensing and recognition of welding environment for intelligent shipyard welding robots *Intelligent Robots and Systems 3: 2159-2165* Kroto H W, Fischer J E, Cox D E 1993 *The Fullerenes* Pergamon:Oxford
- [2] Xu P, Tang X, Yao S 2008 Application of circular laser vision sensor (CLVS) on welded seam tracking *Journal of Materials Processing Technology* **205**(1-3) 404-10
- [3] Huang Y, Xiao Y, Wang P, Li M 2013 A seam-tracking laser welding platform with 3D and 2D visual information fusion vision sensor system *The International Journal of Advanced Manufacturing Technology* **67**(1-4) 415-26
- [4] Kim J S, Son Y T, Cho H S, Wang K, Koh 1995 A robust method for vision-based seam tracking in robotic arc welding *Intelligent Control* doi:10.1109/ISIC.1995.5250
- [5] Chokkalingham S, Chandrasekhar N, Vasudevan M 2012 Predicting the depth of penetration and weld bead width from the infra red thermal image of the weld pool using artificial neural network modeling *Journal of Intelligent Manufacturing* **23**(5) 1995-2001
- [6] Gao X, You D, Katayama S 2012 Infrared image recognition for seam tracking monitoring during fiber laser welding *Mechatronics* **22**(4) 370-80
- [7] Shen H, Lin T, Chen S, Li L 2010 Real-time seam tracking technology of welding robot with visual sensing *Journal of Intelligent & Robotic Systems* **59**(3-4) 283-98
- [8] Xu Y, Lv N, Zhong J 2012 Research on the real-time tracking information of three-dimension welding seam in robotic GTAW Process based on composite sensor technology *Journal of Intelligent & Robotic Systems* **68**(2) 89-103
- [9] Bae K-Y, Lee T-H, Ahn K-C 2002 An optical sensing system for seam tracking and weld pool control in gas metal arc welding of steel pipe *Journal of Materials Processing Technology* **120**(1-3) 458-65
- [10] Ma H, Wei S, Sheng Z, Lin T, Chen S 2010 Robot welding seam tracking method based on passive vision for thin plate proximate-gap butt welding *The International Journal of Advanced Manufacturing Technology* **48**(9-12) 945-53
- [11] Shi Y 2001 A vision-based automatic seam tracking system for underwater flux-cored arc welding *Dissertation, South China University of Technology* (in Chinese)
- [12] Li M, Sun D, Cai Y, Li F, Wu Y 2012 Reach on the image of pool acquisition system based LinLog of Photographic technology *Welding* 1 53-7 (in Chinese)
- [13] Bao S, Zhang K, Wu Y 2008 A detailed analysis of welding arc spectrum distribution characteristics to choose light sources of laser sensors *Journal of Optoelectronics Laser* **20**(4) 504-9 (in Chinese)
- [14] Zheng J, Liu Z, Pan J 2008 Extraction of outline feature points based on the minimum approach error *J Tingshua University (Sci & Tech)* 2 165-8 (in Chinese)

Authors	
	<p><b>Yanming Quan, 1957, China.</b></p> <p><b>Current position, grades:</b> a professor in South China University of Technology, Guangzhou.  <b>Scientific interest:</b> information system, measurement and control technology.</p>
	<p><b>Qilin Bi, 1983, China.</b></p> <p><b>Current position, grades:</b> doctor degree candidate at School of Mechanical &amp; Automotive Engineering in South China University of Technology.  <b>Scientific interest:</b> information system, measurement and control technology.</p>